Responsive Nanoassemblies via Interpolyelectrolyte Complexation of Amphiphilic Block Copolymer Micelles†

Brad S. Lokitz,‡ Anthony J. Convertine,‡ Ryan G. Ezell,‡ Andrew Heidenreich,‡ Yuting Li,‡ and Charles L. McCormick*,‡,§

Department of Polymer Science and Department of Chemistry & Biochemistry, University of Southern Mississippi, Hattiesburg, Mississippi 39406

Received July 24, 2006; Revised Manuscript Received September 29, 2006

ABSTRACT: Shell "locked" nanoassemblies ranging in size from 34 to 78 nm have been prepared from interpolyelectrolyte complexation of block copolymer micelles of poly[(*N*,*N*-dimethylacrylamide)-*b*-(*N*-acryloylalanine)-*b*-(*N*-isopropylacrylamide)] with the homopolymer poly(ar-vinylbenzyl)trimethylammonium chloride above the unimer to micelle phase transition temperature of the block copolymer in water. Of technological significance is the reversibility of the shell cross-linking by addition of 0.4 M NaCl, allowing micelle dissociation below the lower critical solution temperature of the copolymer micelles. Poly(*N*-acryloylalanine) (AAL) and block copolymers were prepared directly in water via controlled reversible addition fragmentation chain transfer (RAFT) polymerization utilizing mono- and difunctional poly(*N*,*N*-dimethylacrylamide) macroCTAs.

Introduction

The ability of well-defined amphiphilic block copolymers to self-assemble into nanostructures such as micelles has attracted a great deal of interest for potential applications in the targeted delivery and controlled release of active agents.[1−13] Self-assembly from unimers to micelles is typically triggered by an external stimulus such as pH, temperature, or added electrolyte and must occur above the critical micelle concentration (cmc) of the block copolymer. Applications in which the micelles undergo dilution can cause the polymer concentration to fall below the cmc and lead to the dissociation of the micelles into unimers. To circumvent this apparent limitation, several groups are currently exploring the covalent stabilization of micelles through chemical cross-links. These covalently stabilized micelles are commonly referred to as shell cross-linked (SCL) micelles and were first reported by Wooley and co-workers in 1996.[14] Several shell cross-linking methods have been reported in the literature including carbodiimide coupling of carboxylic acid groups via diamines,[15,16] quaternization of amino groups,[14,17−19] the reaction of hydroxyl groups with divinyl sulfone,[20] and UV-induced coupling of cinnamoyl groups.[21] Recently, we reported the formation of SCL micelles using the functional monomer *N*-acryloxysuccinimide (NAS) with diamines and the reversible cross-linking of micelles using cystamine as the cross-linking agent.[22,23]

Traditional cross-linking technologies in pharmaceutical and other controlled delivery applications are often limited by a number of factors including poor reagent solubility and low reaction efficiency. Additionally, these reagents are often toxic and must be removed prior to use.[2,13,16,21] An alternative approach involves the complexation of charged segments incorporated into the micelle with oppositely charged polymeric cross-linkers to form polyelectrolyte complexed micelles.[24] Polyelectrolyte complexation is reported to have advantages over traditional cross-linking reactions in that products exhibit low toxicity and physical cross-links are formed without altering the activity of the reactive agent. Additionally, polyelectrolyte complexation produces no byproducts and is reversible in the presence of added salt.[24]

N-Acryloyl derivatives of amino acids can be synthesized in a facile manner by reaction with acryloyl chloride. These functional biomimetic monomers are of interest due to their amphoteric nature, chirality, and ability to self-assemble into high-order structures.[25−28] Rapid developments of controlled radical polymerization techniques now allow the preparation of well-defined functional polymers and block copolymers.[29−31] More specifically, reversible addition fragmentation chain transfer (RAFT)[31−34] polymerization allows for the direct synthesis of several acrylamido and methacrylamido monomers and the formation of complex architectures including well-defined stimuli-responsive block copolymers. For example, our group has reported the aqueous RAFT polymerization and copolymerization of hydrophilic (meth)acrylamido monomers including anionic,[34−36] cationic,[34,37] zwitterionic,[34,38,39] and neutral derivatives.[34,40−45]

Herein we report a facile method for the synthesis of reversible shell "locked" nanoassemblies with solution behavior idealized in Scheme 1. Block copolymers of *N*,*N*-dimethylacrylamide (DMA), *N*-acryloylalanine (AAL), and *N*-isopropylacrylamide (NIPAM) prepared via sequential aqueous RAFT polymerization are shown to undergo a reversible, temperature-induced unimer-to-micelle transition. Above the phase transition temperature, the resulting micelles are cross-linked via interpolyelectrolyte complexation of the poly(AAL) segments in the hydrated shell with the cationic homopolymer poly[(ar-vinylbenzyl)ammonium chloride] (PVBTAC). These interpolyelectrolyte complexed micelles remain intact upon cooling below the lower critical solution temperature. However, of potential technological value is the reversibility of the cross-linking and associated loss of nanostructure integrity with addition of simple electrolytes, in our case 0.4 M NaCl. To our knowledge, this represents not only a unique method of reversible cross-linking but also the first report of the RAFT polymerization of an unprotected amino acid-based monomer directly in water.

† Paper number 125 in a series on Water Soluble Polymers.
‡ Department of Polymer Science.
§ Department of Chemistry & Biochemistry.

10.1021/ma061672y CCC: $33.50 © 2006 American Chemical Society
Published on Web 11/10/2006

Scheme 1. Temperature-Responsive Micellization of Block Copolymers Comprised of *N*,*N*-Dimethylacrylamide (DMA), *N*-Acryloylalanine (AAL), and *N*-isopropylacrylamide (NIPAM) and Reversible Interpolyelectrolyte-Complexed Micelle Formation

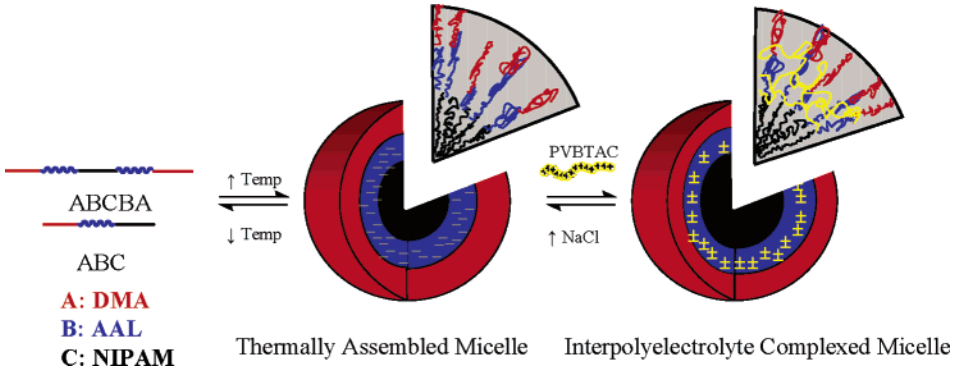

Scheme 2. Synthetic Pathway for the Aqueous Reversible Addition Fragmentation Chain Transfer (RAFT) Polymerization of *N*-Acryloylalanine (AAL) with 4-Cyanopentanoic Acid Dithiobenzoate (CTP) or 2-Ethylsulfanylthiocarbonylsulfonyl-2-methylpropionic Acid (EMP) and 4,4′-Azobis(4-cyanopentanoic acid) V-501 as the Free Radical Initiator

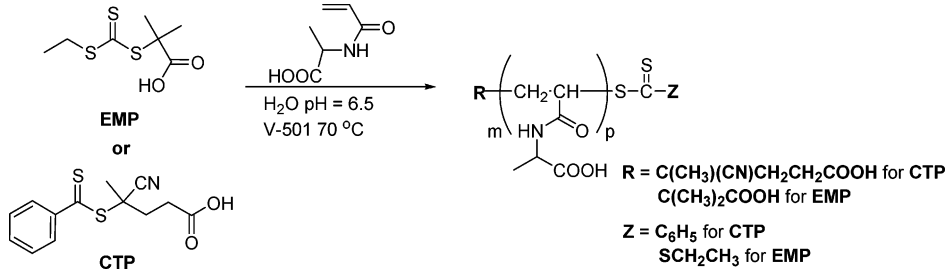

Table 1. [Monomer]/[Chain Transfer Agent] Initial Concentrations ($[M]_0/[CTA]_0$), Percent Conversion, Number-Average Molecular Weight, and Polydispersity (M_w/M_n) Data for the Aqueous Reversible Addition Fragmentation Chain Transfer (RAFT) Polymerization of *N*-Acryloylalanine (AAL) at 70 °C Mediated by 4-Cyanopentanoic Acid Dithiobenzoate (CTP) and 2-Ethylsulfanylthiocarbonylsulfonyl-2-methylpropionic Acid (EMP) with Initial [Chain Transfer Agent]:[Initiator] Ratio ($[CTA]_0:[I]_0$) of 5:1

entry	CTA	$[M]_0/[CTA]_0$	time (min)	conv (%)[b]	M_n (g mol^{-1})[c]	$M_{n,th}$ (g mol^{-1})	M_w/M_n[c]
1			15	gel			
2	CTP	70	105	16	4100	1600	1.29
3	CTP	70	195	88	11800	8800	1.16
4	CTP	210	45	3.0	3200	900	1.27
5	CTP	210	300	63	24000	18988	1.15
6	CTP	420	115	13	12800	7800	1.24
7	CTP	420	210	81	52200	48600	1.18
8	CTP	630	125	9.0	15000	8100	1.22
9	CTP	630	225	83	76600	74700	1.19
10	EMP	70	9	14	3600	1400	1.25
11	EMP	70	45	95	10600	9500	1.14
12	EMP	210	15	13	6100	3900	1.24
13	EMP	210	45	93	30400	27900	1.11
14	EMP	420	15	5.0	7000	3000	1.26
15	EMP	420	60	80	51250	48000	1.07
16	EMP	630	25	15	19800	13500	1.20
17	EMP	630	45	73	71500	65700	1.03

[a] Polymers synthesized at 70 °C at 1 M monomer in H_2O (pH = 6.5) under a nitrogen atmosphere with V-501 as the initiator. [b] Conversions were determined using RI peak intensity by comparing the area of the monomer peak at time *t* to the area of the monomer peak at time 0. [c] As determined by aqueous size exclusion chromatography (ASEC).

Experimental Section

Materials. All reagents were purchased from Aldrich at the highest purity available and used as received unless otherwise stated. 4-Cyanopentanoic acid dithiobenzoate (CTP) and 2-ethylsulfanylthiocarbonylsulfonyl-2-methylpropionic acid (EMP) were synthesized according to literature procedures.[43,44] Mono- and difunctional macroCTAs of *N*,*N*-dimethylacrylamide and PVBTAC (M_n = 26 000 g/mol, M_n/M_w = 1.21) were prepared as previously described.[34,41] 2-(1-Carboxy-1-methylethylsulfanylthiocarbonylsulfanyl)-2-methylpropionic acid (CMP) was donated by Noveon and was recrystallized from hexanes. 4,4′-Azobis(4-cyanopentanoic acid) (V-501) and 4,4′-azobis[2-(imidazolin-2-yl)propane] dihydrochloride (VA-044) were donated by Wako Chemicals and were recrystallized twice from methanol prior to use. NIPAM was recrystallized twice from hexanes prior to use.

Synthesis of *N*-Acryloylalanine (AAL). The synthesis of the alanine-based acrylamido monomer, *N*-acryloyolalanine (AAL), was performed as follows: L-Alanine (0.4 mol, 35.43 g) and NaOH (0.8 mol, 32.01 g) were dissolved in DI water (180 mL) and stirred using a mechanical stirrer. Once the solids had completely dissolved, the solution was cooled to 4 °C using an ice bath. Acryloyl chloride (0.4 mol, 36.18 g) was added dropwise over 2 h, maintaining the temperature of the reaction at 4 °C. Upon complete addition of acryloyl chloride, HCl was added dropwise to neutralize the monomer and induce precipitation. The afforded crystals were then collected by filtration and recrystallized from water. Melting point 162−164 °C (reported literature mp 163 °C).[46] ^{1}H NMR: C*H*$_2$-CHCO 5.71 (d), CH_2C*H*CO 6.33 (m), HNC*H*(COOH)CH_3 4.45 (m), HNCH(COOH)C*H*$_3$ 2,17 (d).

General Procedure for the RAFT Polymerization of AAL. Polymerizations were conducted at 70 °C, employing V-501 as the primary radical source and CTP or EMP as the RAFT CTA. Polymerizatoins were performed directly in water (pH 6.5) with an initial monomer concentration ($[M]_0$) of 1.0 M in individual, septa-sealed vials, which were purged with nitrogen at 5 °C for 30 min prior to the reaction. The initial monomer to CTA ratio ($[M]_0/[CTA]_0$) was varied between 70 and 630 while the initial CTA to initiator ratio ($[CTA]_0/[I]_0$) was held constant at 5:1. For example, entry 3 (Table 1) was prepared by reacting 1.43 g (0.001 mol) of AAL with 39.99 mg (1.43×10^{-4} mol) of CTP and 8.02 mg (2.86×10^{-5} mol) of V-501 in 10 mL of water for 195 min. The polymerization kinetics and the absolute molecular weights were determined from aliquots (0.5 mL) taken at predetermined time intervals and quenched via rapid cooling and exposure to oxygen.

Block Copolymer Synthesis. A macroCTA of DMA was used for preparing di- and triblock copolymers of DMA-*b*-AAL and DMA-*b*-AAL-*b*-DMA. The polymerizations were conducted directly in water (pH 6.5) with an initial monomer concentration of 1 M at 70 °C with V-501 as the initiator. The $[PDMA]_0$:$[V\text{-}501]_0$ ratio was maintained at 5:1, and the target DP for AAL was 105. For example, DMA_{100}-*b*-AAL_{65} was prepared by reacting 1.43 g (0.001 mol) of AAL with 1.43 g (1.43×10^{-4} mol) of DMA_{100} macroCTA and 9.26 mg (2.86×10^{-5} mol) of V-501 in 10 mL of water for 45 min. The DMA-*b*-AAL diblock and DMA-*b*-AAL-*b*-DMA triblock macroCTAs were subsequently chain extended with NIPAM to produce tri- and pentablock copolymers of DMA-*b*-AAL-*b*-NIPAM and DMA-*b*-AAL-*b*-NIPAM-*b*-AAL-*b*-NIPAM. The polymerizations were conducted directly in water (pH 5.5) with an initial monomer concentration of 1 M at 25 °C with VA-044 as the initiator. The $[macroCTA]_0$:$[VA\text{-}044]_0$ ratio was maintained at 3:1, and the target degree of polymerization (DP) for NIPAM was varied. For example, DMA_{100}-*b*-AAL_{65}-*b*-$NIPAM_{61}$ was prepared by reacting 1.13 g (0.001 mol) of NIPAM with 2.80 g (1.41×10^{-4} mol) of DMA_{100}-*b*-AAL_{65} macroCTA and 15.24 mg (4.72×10^{-5} mol) of VA-044 in 10 mL of water for 180 min. Polymerizations were conducted under a nitrogen atmosphere in round-bottomed flasks equipped with magnetic stir bars and sealed with rubber septa. The products were purified by dialysis against deionized water and isolated by lyophilization.

Preperation of Micelles. Copolymers were dissolved directly into an aqueous solution (pH = 6.8 ± 0.2) containing 0.01 M NaCl (HPLC grade water) (1 mg/mL, 10 mL). Micellization of the copolymers was achieved by raising the solution temperature above the LCST of the NIPAM block.

Interpolyelectrolyte Cross-Linked Micelles. Shell cross-linked micelles were prepared from an aqueous stock solution of the copolymer (1 mg/mL, 3 mL). The pH of the solution was adjusted to 9.0 ± 0.2 and allowed to equilibrate at 50 °C for 30 min. Poly([ar-vinylbenzyl]trimethylammonium chloride) (PVBTAC), a cationic polymer (M_n = 26 000 g/mol, M_n/M_w = 1.21), was then added at a 1:1 mole ratio based on the carboxylic acid groups of AAL. The micelle solution was then stirred at 50 °C for 15 min.

Aqueous Size Exclusion Chromatography. Homopolymers of AAL, DMA-*b*-AAL, and DMA-*b*-AAL-*b*-DMA were analyzed directly by aqueous size exclusion chromatography (ASEC) using an aqueous eluent of 20% acetonitrile/80% 0.5 M Na_2SO_4. DMA-*b*-APA-*b*-NIPAM and DMA-*b*-AAL-*b*-NIPAM-*b*-AAL-*b*-DMA copolymers were analyzed directly by ASEC using an aqueous eluent of 0.1 M $NaNO_3$. A flow rate of 0.5 mL/min at 25 °C, TOSOH Biosciences TSK-GEL columns [G3000 PWXL (<50 000 g mol^{-1}, 200 Å) and G4000 PWXL (2000−300 000 g mol^{-1}, 500 Å)], a Polymer Labs LC 1200 UV/vis, Wyatt Optilab DSP interferometric refractometer, and Wyatt DAWN EOS multiangle laser light scattering detectors (690 nm) were used. Wyatt DNDC for windows was used for d*n*/d*c* determinations.

^{1}H NMR Spectroscopy. ^{1}H NMR spectra were recorded with a temperature-controlled Mercury Innova 500 MHz spectrometer. Samples were prepared as 2% w/w solutions in D_2O (HOD internal standard). Copolymer compositions were determined by a comparison of resonances associated with the comonomers.

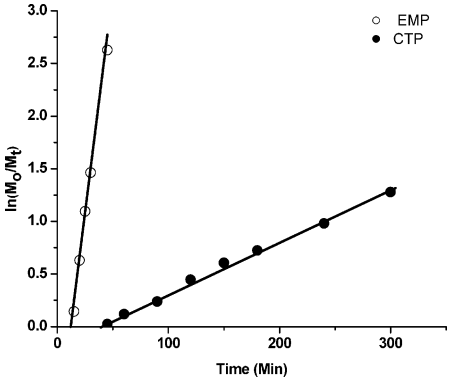

Figure 1. Pseudo-first-order kinetic plot for the 4-cyanopentanoic acid dithiobenzoate (CTP) and 2-ethylsulfanylthiocarbonylsulfonyl-2-methylpropionic acid (EMP) mediated hompolymerizations of *N*-acryloylalanine (AAL) at 70 °C.

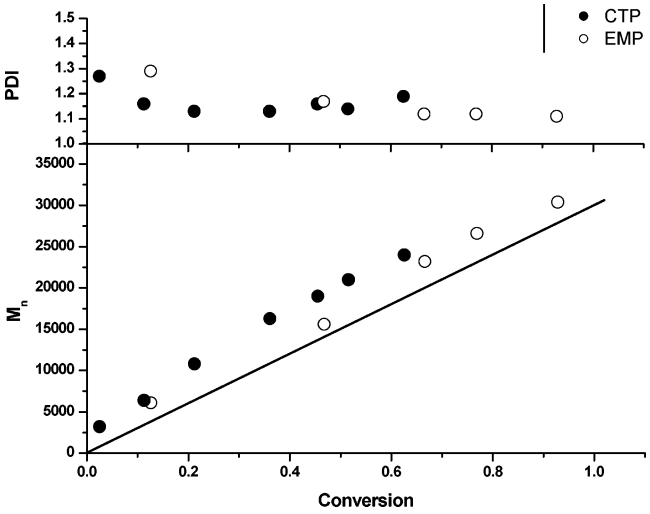

Figure 2. Number-average molecular weight (M_n) and PDI (M_w/M_n) vs conversion for the aqueous homopolymerizations of *N*-acryloylalanine (AAL) mediated by 4-cyanopentanoic acid dithiobenzoate (CTP) and 2-ethylsulfanylthiocarbonylsulfonyl-2-methylpropionic acid (EMP) at 70 °C.

Light Scattering Measurements. Static light scattering measurements were performed on a Malvern Instruments Zetasizer Nano ZS using a constant scattering angle of 173°. The apparent micellar molar mass (M_w) and second virial coefficient (A_2) were estimated from the relationship

$$KC_p/R_\theta = (1/M_w + 2A_2C_p)$$

where K, C_p, M_W, R_θ, and A_2 are the optical constant, polymer concentration, molecular weight, Rayleigh ratio, and second virial coefficient, respectively. By measuring R_θ at a series of polymer concentrations ($C_{polymer} \approx C_{micelle}$) apparent values, M_w and A_2 were obtained from Debye plots.

Dynamic Light Scattering. Dynamic light scattering studies of the copolymers at concentrations of 1.00 g/L in an aqueous 0.01 M NaCl solution were conducted using a Malvern Instruments Zetasizer Nano ZS instrument equipped with a 4 mW He−Ne laser operating at λ = 633 nm, an avalanche photodiode detector with high quantum efficiency, and an ALV/LSE-5003 multiple tau digital correlator electronics system.

Zeta Potential. The zeta potentials of the thermally responsive and SCL micelle solutions (1 mg/mL, 10 mL) at pH 9.0 ± 0.2 were determined using a Malvern Instruments Zetasizer Nano ZS instrument at 50 and 25 °C, respectively.

Transmission Electron Microscopy. Transmission electron microscopy (TEM) measurements were conducted using a JEOL JEM-2100 electron microscope at an acceleration voltage of 200

Scheme 3. Synthetic Route for Preparation of ABC (Pathway A) and ABCBA (Pathway B) Copolymers of *N,N*-Dimethylacrylamide (DMA), *N*-Acryloylalanine (AAL), and *N*-Isopropylacrylamide (NIPAM) via Aqueous Reversible Addition Fragmentation Chain Transfer (RAFT) Polymerization[a]

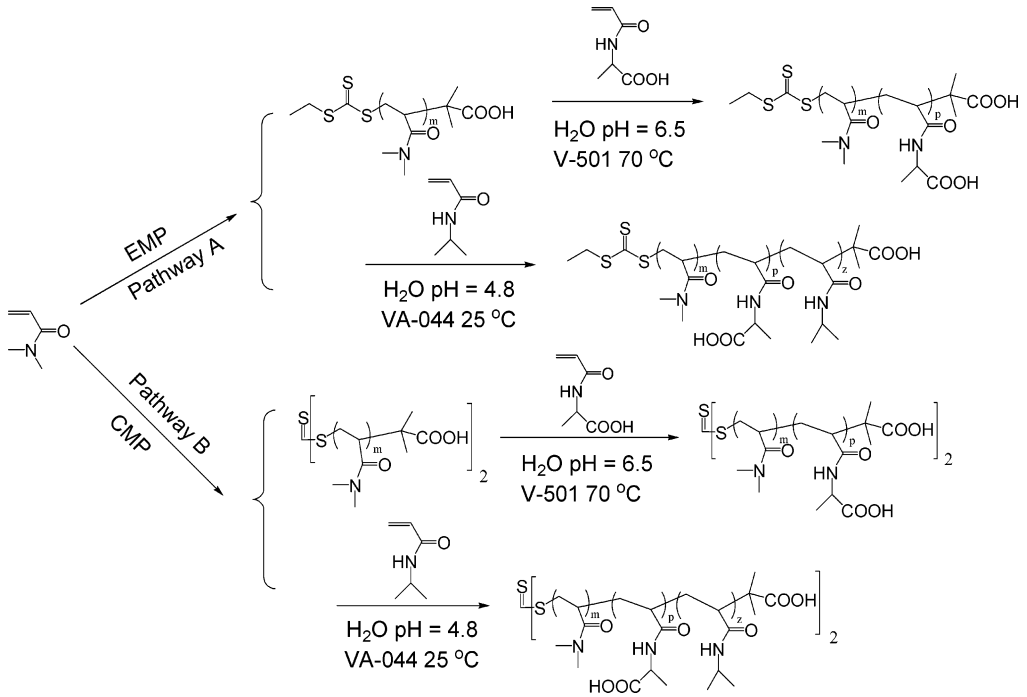

[a] 2-Ethylsulfanylthiocarbonylsulfonyl-2-methylpropionic acid (EMP) (pathway A) and 2-(1-carboxy-1-methylthylsulfanylthiocarbonylsulfanyl)-2-methylpropionic acid (CMP) (pathway B) were used as the chain transfer agents and 4′-azobis[2-(imidazolin-2-yl)propane] dihydrochloride (VA-044) and 4,4′-azobis(4-cyanopentanoic acid) V-501 as the free radical initiators.

kV. The specimens were prepared by placing a 10 μL drop of the 0.005% w/w micelle solution on a Formvar-coated copper grid followed by water evaporation.

Results and Discussion

Aqueous RAFT Polymerization of AAL. *N*-Acryloylalanine was selected for this study on the basis of its facile synthesis from readily available amino acid sources and its amphoteric nature that allows polymerization, purification, and characterization directly in aqueous solution. To show the viability of block formation, the RAFT polymerization of AAL was first performed directly in water as a control experiment using V-501 as the free radical initiator and 4-cyanopentanoic acid dithiobenzoate (CTP) or 2-ethylsulfanylthiocarbonylsulfonyl-2-methylpropionic acid (EMP) as the chain transfer agent (CTA) (Scheme 2).

Shown in Figure 1 are the pseudo-first-order kinetic plots for the CMP/EMP-mediated hompolymerizations of AAL at 70 °C with an initial monomer to CTA ratio ($[M]_0/[CTA]_0$) of 210/1. Linear pseudo-first-order kinetics plots are obtained for both CTAs, and the apparent rate of polymerization of EMP is significantly higher than that of CTP, the result of a higher rate of fragmentation of the intermediate radical species during the RAFT process.[45]

The faster rate of polymerization and the maintenance of pseudo-first-order kinetics to higher conversions and the closer agreement of M_n to theoretically predicted values, while maintaining low PDI values shown in Figure 2, favor the use of EMP under our experimental conditions. The PDI vs conversion for the CTP/EMP polymerizations of AAL indicates that both CTAs provide good overall control of the reaction with M_w/M_n values less than 1.2 at high conversions. Given the low polydispersities and the linear increase in molecular weight with conversion, it is clear that both CTAs allow for the controlled synthesis of AAL directly in water.

To further show the molecular weight control with our system, the initial monomer to CTA ratio ($[M]_0/[CTA]_0$) was varied to target degrees of polymerization of 70, 210, 420, and 630. The experimental data are summarized in Table 1, indicating that the polymers possess low PDIs (<1.3), and experimental molecular weights in good agreement with those theoretical molecular weights targeted.

Thermally Responsive Block Copolymers. Having established conditions for controlled/"living" polymerization of AAL, we constructed thermally responsive triblock and pentablock copolymers as detailed in the Experimental Section and shown in Scheme 3. The initial hydrophilic, neutral block was synthesized from DMA utilizing CMP or EMP as chain transfer agents to generate the mono- (pathway A) or difunctional (pathway B) macroCTAs with respective M_n (M_w/M_n) values of 9900 g/mol (1.07) and 10 500 g/mol (1.04).[44] Subsequent sequential block copolymerization with AAL and then with NIPAM yielded the triblock and pentablock samples utilized in our micellization and cross-linking studies.

Structural data shown in Table 2 for these samples were determined by utilizing NMR and aqueous size exclusion chromatography with multiangle laser light scattering (ASEC-MALLS) detection.

^{1}H NMR spectra for the DMA macroCTA and the subsequent di- and triblock copolymers are shown in Figure 3. Block copolymer compositions were determined by comparing resonances of the DMA dimethyl group (~2.8 ppm) to those associated with the AAL methyl (1.1 ppm) and NIPAM methine (4.2 ppm).

Shown in Figure 4 are (A) the normalized ASEC chromatograms and (B) cumulative weight fractions for the monofunctional DMA macroCTA and the resultant DMA_{100}-*b*-AAL_{65} copolymer. Near-quantitative blocking efficiency (percentage of macroCTA converted to block copolymer) was confirmed

Table 2. Degree of Polymerization (DP), Number-Average Molecular Weight (M_n), and Polydispersity (M_w/M_n) Data for ABC and ABCBA Copolymers *N,N*-Dimethylacrylamide (DMA) A Block, *N*-Acryloylalanine (AAL) B Block, and *N*-Isopropylacrylamide (NIPAM) C Block

sample	DP DMA[a]	DP AAL[b]	DP NIPAM[b]	M_n (g mol^{-1})[a]	M_w/M_n[a]
$DMA_{100}AAL_{65}NIPAM_{61}$	100	65	61	26 000	1.15
$DMA_{100}AAL_{65}NIPAM_{165}$	100	65	165	37 300	1.14
$DMA_{53}AAL_{38}NIPAM_{194}AAL_{38}DMA_{53}$	106	76	194	43 400	1.18
$DMA_{53}AAL_{38}NIPAM_{345}AAL_{38}DMA_{53}$	106	76	345	60 400	1.16

[a] As determined by aqueous size exclusion chromatography (ASEC). [b] Determined by proton nuclear magnetic resonance (^{1}H NMR) spectroscopy in D_2O.

Table 3. Apparent Hydrodynamic Diameter (D_h), Critical Micelle Temperature (cmt), Apparent Micelle Molar Mass (M_w), and Second Virial Coefficient (A_2) Determined by Static and Dynamic Light Scattering

sample	D_h 25 °C (nm)	D_h 50 °C (nm)	cmt (°C)	$M_w \times 10^{-6}$ (g mol^{-1}) at 50 °C	$A_2 \times 10^5$ (mL mol/g^2) at 50 °C
$DMA_{100}AAL_{65}NIPAM_{61}$	8.8	34.7	47	0.396	0.144
$DMA_{100}AAL_{65}NIPAM_{165}$	10.4	42.7	36	2.18	8.91
$DMA_{53}AAL_{38}NIPAM_{194}AAL_{38}DMA_{53}$	10.2	39.9	36	1.98	9.13
$DMA_{53}AAL_{38}NIPAM_{345}AAL_{38}DMA_{53}$	13.1	85.9	34	7.50	8.55

Table 4. Apparent Hydrodynamic Diameter (D_h) and Zeta Potential (ξ) for the Ionically Interpolyelectrolyte Complexed Micelles

sample	D_h 50 °C (nm)	D_h 25 °C (nm)	ξ (mV) 50 °C no PVBTAC	ξ (mV) 25 °C SCL
$DMA_{100}AAL_{65}NIPAM_{61}$	34.7	34.1	−31.2	−0.2
$DMA_{100}AAL_{65}NIPAM_{165}$	42.7	37.4	−32.9	−2.4
$DMA_{53}AAL_{38}NIPAM_{194}AAL_{38}DMA_{53}$	39.9	42.1	−33.0	−1.4
$DMA_{53}AAL_{38}NIPAM_{345}AAL_{38}DMA_{53}$	85.9	78.6	−38.5	−3.4

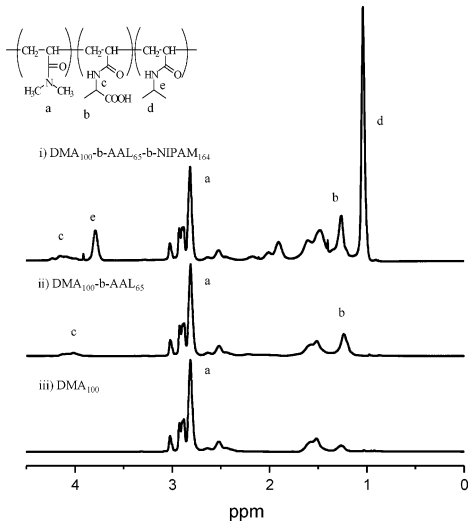

Figure 3. Proton nuclear magnetic resonance (^{1}H NMR) spectra for block copolymers of *N,N*-dimethylacrylamide (DMA), *N*-acryloylalanine (AAL), and *N*-isopropylacrylamide (NIPAM): DMA_{100}-*b*-AAL_{65}-*b*-$NIPAM_{165}$ (i), DMA_{100}-*b*-AAL_{65} (ii), and DMA_{100} (iii).

by the shift in the ASEC trace (RI detector) to higher elution volume and the shift of the near-monodisperse distribution to higher molecular weight. Shown in Figure 4C are the normalized ASEC chromatograms for the ABC triblock copolymer DMA_{100}-*b*-AAL_{65}-*b*-$NIPAM_{164}$ and the ABCBA pentablock copolymer DMA_{53}-*b*-AAL_{38}-*b*-$NIPAM_{345}$-*b*-AAL_{38}-*b*-DMA_{53}.

ABC triblock and ABCBA pentablock copolymers with different targeted degrees of polymerization for the NIPAM containing C block (Table 2) were utilized in our experiments to demonstrate thermally reversible micellization and interpolyelectrolyte shell cross-linking (Scheme 1).

Temperature-Induced Micellization. Temperature-induced micellization can be followed using dynamic light scattering. Above its LCST, poly(NIPAM) becomes dehydrated as a result of an entropy gain resulting from the release of water molecules upon association of the isopropyl groups.[47,48] The dehydration of the NIPAM block causes the block copolymers to undergo a temperature-induced transition from molecularly dissolved unimers to aggregates above the critical micelle temperature (cmt). At the cmt, a large increase in the hydrodynamic diameter of the block copolymers occurs followed by a decrease in size as the solution temperature is increased further. The decrease in micelle size with increasing temperature is most evident for the pentablock copolymer DMA_{53}-*b*-AAL_{38}-*b*-$NIPAM_{345}$-*b*-AAL_{38}-*b*-DMA_{53} and can be attributed to its longer NIPAM block. The copolymer exists in the unimer state with an average hydrodynamic diameter of 13.2 nm below the cmt. As the temperature is further increased above the cmt, the unimers associate to form aggregates of 250 nm before reaching an equilibrium size of 85.9 nm. By contrast, DMA_{100}-*b*-AAL_{65}-*b*-$NIPAM_{61}$ shows the smallest change in hydrodynamic diameter with increasing temperature which is related to its short NIPAM block length. Here the hydrodynamic diameter of the copolymer increases from unimers of 8.8 nm to aggregates of 36.3 nm at the cmt and 34.7 nm at 50 °C. Yusa and co-workers attributed this decrease in size above the cmt to either a decrease in the aggregation number of the aggregates or further dehydration of the NIPAM blocks.[49] Figure 5 shows the temperature-induced changes in the hydrodynamic volume for an aqueous solution of the respective block copolymer micelles.

The cmt for the block copolymers decreases when the NIPAM block length increases. This is evidenced by the copolymer with the shortest NIPAM block length, DMA_{100}-*b*-AAL_{65}-*b*-$NIPAM_{61}$, having the highest cmt (47 °C) while the copolymer with the largest NIPAM block length, DMA_{53}-*b*-AAL_{38}-*b*-$NIPAM_{345}$-*b*-AAL_{38}-*b*-DMA_{53}, has the lowest cmt (34 °C). These results are consistent with reports by Liu et al.[50] and Xia and co-workers,[51] who saw a decrease in the phase transition temperature for a series of NIPAM homopolymers. The hydrodynamic diameter for the block copolymer series follows the trend we recently reported in which the micelle size is shown to increase with increasing NIPAM content.[44] In the current study, the micelles range from 34.7 nm for DMA_{100}-*b*-AAL_{65}-*b*-$NIPAM_{61}$ to 85.9 nm for DMA_{53}-*b*-AAL_{38}-*b*-$NIPAM_{345}$-*b*-AAL_{38}-*b*-DMA_{53} (Table 3). The block architecture appears to have little effect on the size of the micelles as DMA_{100}-*b*-AAL_{65}-*b*-$NIPAM_{164}$ and DMA_{53}-*b*-AAL_{38}-*b*-$NIPAM_{194}$-*b*-AAL_{38}-*b*-DMA_{53} have similar sizes of 42.7 and 39.9 nm, respectively.

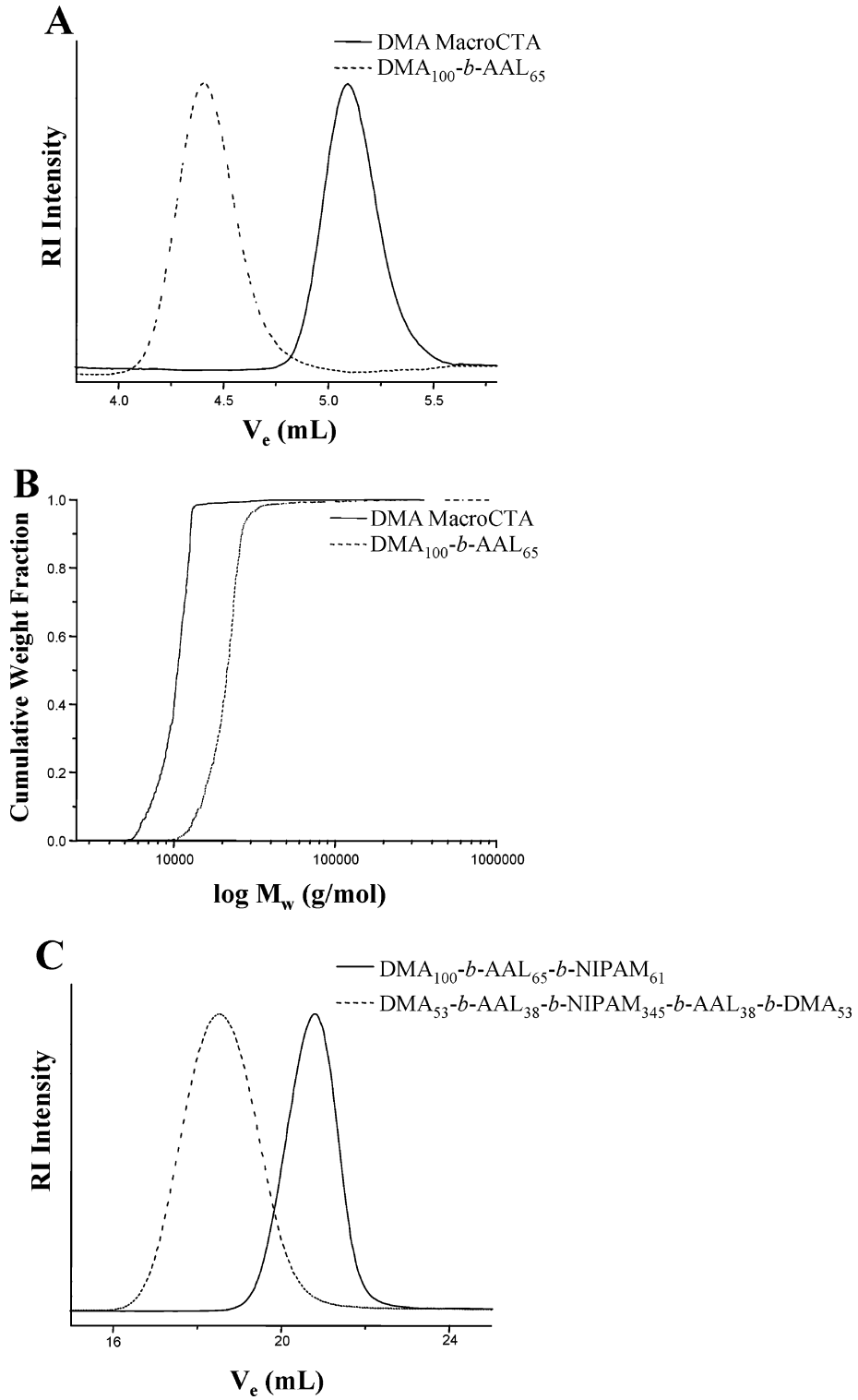

Figure 4. (A) Refractive index (RI) traces and (B) cumulative weight fractions for the chain extension of the *N*,*N*-dimethylacrylamide (DMA) macro-chain-transfer agent (macroCTA) (—, DMA macroCTA, number-average molecular weight (M_n) = 9900 g/mol; polydispersity (M_w/M_n = 1.07) with *N*-acryloylalanine (AAL) (- - -, DMA_{100}-*b*-AAL_{65}, M_n = 20 100 g/mol; M_w/M_n = 1.13) showing the evolution of molar mass with time. (C) RI traces for the ABC triblock copolymer of of DMA, AAL, and *N*-isopropylacrylamide (NIPAM) (—, DMA_{100}-*b*-AAL_{65}-*b*-$NIPAM_{164}$, M_n = 28 400 g/mol; M_w/M_n = 1.18) and the ABCBA pentablock copolymer (- - -, DMA_{53}-*b*-AAL_{38}-*b*-$NIPAM_{345}$-*b*-AAL_{38}-*b*-DMA_{53}, M_n = 60 400 g/mol; PDI = 1.16).

That polydispersities of the micelles decrease with increasing NIPAM content is apparent by comparing the distribution of $DMA_{100}AAL_{65}NIPAM_{61}$ (0.153) with that of $DMA_{100}AAL_{65}$-$NIPAM_{165}$ (0.075) and the distribution of $DMA_{53}AAL_{38}$-$NIPAM_{194}AAL_{38}DMA_{53}$ (0.121) with that of $DMA_{53}AAL_{38}$-$NIPAM_{345}AAL_{38}DMA_{53}$ (0.010). These data are consistent with our previous report.[22]

Interpolyelectrolyte Cross-Linking. Thermally assembled micelles were ionically cross-linked (Scheme 3) by allowing the micelle solution to equilibrate at 50 °C for 30 min before adding a predetermined amount (1:1 mole ratio anionic:cationic repeat units) of a 0.1% (w/w) solution of the RAFT polymerized cationic polymer VBTAC (M_n = 26 000 g/mol, M_n/M_w = 1.21). If shell cross-linking had not occurred, dissociation into

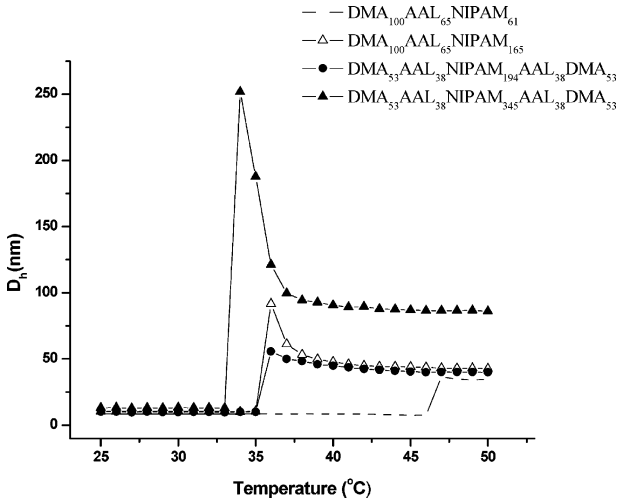

Figure 5. Apparent hydrodynamic diameters (D_h) for the block copolymers of *N*,*N*-dimethylacrylamide (DMA), *N*-acryloylalanine (AAL), and *N*-isopropylacrylamide (NIPAM) measured by dynamic light scattering (polymer concentration = 1.0 g/L) as a function of temperature.

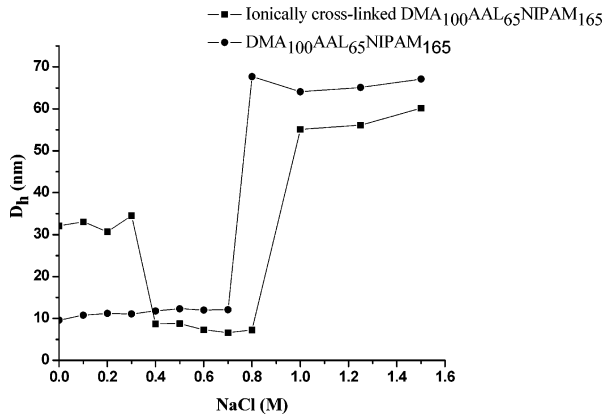

Figure 6. Apparent hydrodynamic diameters (D_h) for the ionically cross-linked micelles and copolymer comprised of *N*,*N*-dimethylacrylamide (DMA), *N*-acryloylalanine (AAL), and *N*-isopropylacrylamide (NIPAM) (DMA_{100}-*b*-AAL_{65}-*b*-$NIPAM_{165}$, polymer concentration = 1.0 g/L) as a function of sodium chloride concentration ([NaCl]).

unimers would be expected upon lowering the solution to 25 °C; however, DLS experiments show that micelles remain intact at room temperature, thus indicating the formation of interpolyelectrolyte cross-linked micelles. The hydrodynamic diameters and zeta potentials for the SCL micelles are shown in Table 4.

In general, a slight decrease in the micelle size is observed upon allowing the solution to cool to room temperature. This is attributed to the neutralization of the AAL block which would minimize the electrostatic repulsion of the carboxyl groups and allow the chains to pack closer together. This would offset the increase in size that would be expected by the rehydration of the NIPAM blocks and result in the overall decrease of the hydrodynamic diameter of the micelles. Generally, particles with zeta potentials $\geq \pm 30$ are considered stable.[52] At 50 ° C, the zeta potentials measured at the micelles surface (corona comprised of DMA and alanine) are in excess of −30 mV, indicating the stability and net negative charge of the micelles. Upon addition of stoichiometric quantities PVBTAC to the amino acid block of the micelles, the zeta potential reached near zero values, suggesting that the micelles are close to their isoelectric point (IEP). The stability of the SCL micelles was investigated using DLS over a temperature (10−70 °C) and pH (2−14) range. The data indicate that the micelles are stable over

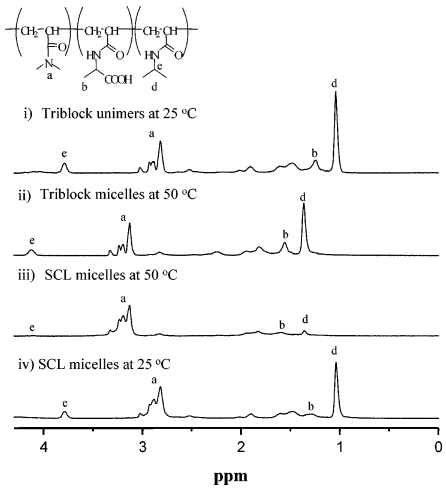

Figure 7. ^{1}H NMR spectra (2% w/w in D_2O) for copolymers comprised of *N*,*N*-dimethylacrylamide (DMA), *N*-acryloylalanine (AAL), and *N*-isopropylacrylamide (NIPAM)−DMA_{100}-*b*-AAL_{65}-*b*-$NIPAM_{165}$ unimers at 25 °C (i), DMA_{100}-*b*-AAL_{65}-*b*-$NIPAM_{165}$ micelles at 50 °C (ii), DMA_{100}-*b*-AAL_{65}-*b*-$NIPAM_{165}$ interpolyelectrolyte complexed micelles at 50 °C (iii), and DMA_{100}-*b*-AAL_{65}-*b*-$NIPAM_{165}$ interpolyelectrolyte complexed micelles at 25 °C (iv).

the examined ranges as no dissociation into unimers is observed. The stability is attributed to the DMA corona providing sufficient steric stabilization and hydrophilicity to keep the micelles dispersed in aqueous solution. In addition, the stability/reversibility of the ionically cross-linked micelles in the presence of added salt was investigated. Figure 6 shows the hydrodynamic diameters of the ionically cross-linked micelles and copolymer comprised of DMA_{100}-*b*-AAL_{65}-*b*-$NIPAM_{165}$ in the presence of NaCl.

The micelles remain intact at salt concentrations as high as 0.3 M NaCl while dissociation into unimers is observed at 0.4 M NaCl, demonstrating the reversibility of the ionic cross-links. It is interesting to note that at 1.0 M NaCl aggregates are once again observed. We have attributed this to the "salting-out" of the NIPAM block. To test this hypothesis, the salt response of the copolymer DMA_{100}-*b*-AAL_{65}-*b*-$NIPAM_{165}$ was investigated. At 25 °C and a concentration of 0.1% w/w the diblock copolymer exists as unimers with diameters of 9.6 nm in water. Increasing the ionic strength of the solution leads to the formation of aggregates with average diameters of ∼65 nm at 0.8 M NaCl, confirming that the addition of salt can render NIPAM blocks hydrophobic enough to induce micellization. The ^{1}H NMR spectra shown in Figure 7 also support the temperature-induced association and ionic cross-linking.

The transition from unimers to micelles can be followed by monitoring the changes in peak intensity with temperature.[24,44,49,50,53] Spectrum (i) represents the triblock copolymer DMA_{100}-*b*-AAL_{65}-*b*-$NIPAM_{165}$ at 25 °C which is present as molecularly dissolved unimers, and the peaks associated with each block are present. Upon raising the solution temperature to 50 °C (ii), the signals labeled "d" and "e" associated with the methyl and methine protons of PNIPAM become broadened and attenuated relative to the PDMA methyl signal "a" and the AAL methyl signal "b", indicating reduced mobility and solvation. This is in agreement with the DLS results which show the presence of aggregates of 42.70 nm. Upon the addition of the cationic cross-linker (iii), peak "b", associated with the methyl group of AAL, also is broadened and attenuated relative to the PDMA methyl peak, indicating its reduced mobility and solvation as a result of polyelectrolyte complexation. When the temperature of the SCL micelle solution (iii) is lowered to 25

CDV

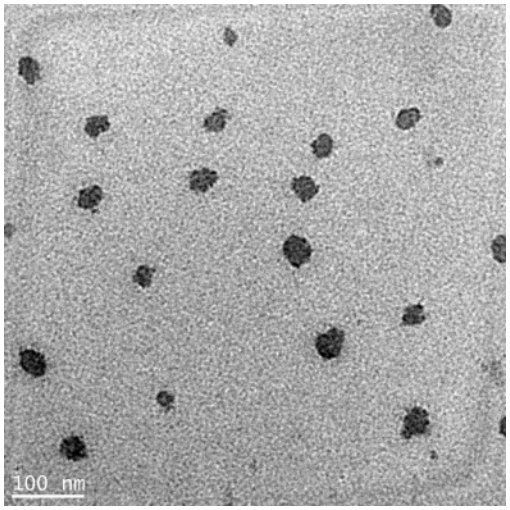

Figure 8. Transmission electron microscopy (TEM) image of interpolyelectrolyte complexed polymeric micelles of *N*,*N*-dimethylacrylamide (DMA), *N*-acryloylalanine (AAL), and *N*-isopropylacrylamide (NIPAM) (DMA_{100}-*b*-AAL_{65}-*b*-$NIPAM1_{165}$) with the cationic polymer poly(ar-vinylbenzyl)trimethylammonium chloride (PVBTAC).

°C (iv), an increase in intensity for the methyl and methine signals of PNIPAM, peaks "d" and "e", while the methyl peak, "b", of AAL remains suppressed, indicating that SCL micelles have been formed.

The self-assembled morphology of the block copolymers was investigated by transmission electron microscopy (TEM). Figure 8 shows the TEM image of interpolyelectrolyte cross-linked micelles formed from the triblock copolymer DMA_{100}-*b*-AAL_{65}-*b*-$NIPAM_{61}$. The image clearly shows uniform micelles with diameters between 30 and 40 nm, which is in reasonable agreement with that of 34.1 nm determined by DLS.

Conclusions. In this work we have shown the controlled polymerization of AAL directly in water utilizing RAFT. Both CTP and EMP afford excellent control of the polymerizations molecular weight and molecular weight distribution. Low polydispersities (<1.19) are achieved at conversions in excess of 80%. The amino acid-based monomer was then incorporated into ABC triblock and ABCBA pentablock copolymers for the facile preparation of thermally responsive, polyelectrolyte cross-linkable micelles. The hydrophilic block length was kept constant while the thermally responsive NIPAM block was varied to investigate the temperature-dependent micellization of the block copolymers. It was shown that the critical micellization temperatures for the block copolymers were directly related to the NIPAM block length as DMA_{100}-*b*-AAL_{65}-*b*-$NIPAM_{61}$ exhibited a transition at 47 °C while the cmt for DMA_{53}-*b*-AAL_{38}-*b*-$NIPAM_{345}$-*b*-AAL_{38}-*b*-DMA_{53} was 34 °C. The size and molecular weight of the micelles were shown to increase with increasing NIPAM block lengths. The cationic polymer VBTAC was employed for the in-situ formation of SCL micelles via interpolyelectrolyte complexation. DLS and TEM were used to confirm the presence of thermodynamically stable micelles. The ionically cross-linked micelles were shown to be reversible in the presence of 0.4 M NaCl. Increasing the salt concentration above 1.0 M NaCl led to the "salting-out" of the NIPAM block and the re-formation of aggregates. The facility by which these nanocomplexes can be formed and the reversibility of these interpolyelectrolyte complexed micelle assemblies suggest that such systems may have potential application in targeted delivery and controlled release of active agents.

Acknowledgment. The Department of Energy (DE-FC26-01BC15317), Genzyme, MRSEC program of the National Science Foundation (DR-0213883), and the Robert M. Hearin Foundation are gratefully acknowledged for financial support. We also thank Noveon donating the chain transfer agent CMP and Wako Chemicals for donating V-501 and VA-044.

References and Notes

(1) Wooley, K. L. *J. Polym. Sci., Part A*: *Polym. Chem.* **2000**, *38*, 1397−1401.
(2) Thurmond, K. B.; Kowalewski, T.; Wooley, K. L. *J. Am. Chem. Soc.* **1997**, *119*, 6656−6665.
(3) Huang, H.; Remsen, E. E.; Wooley, K. L. *Chem. Commun.* **1998**, 1415−1416.
(4) Huang, H.; Remsen, E. E.; Kowalewski, T.; Wooley, K. L. *J. Am. Chem. Soc.* **1999**, *121*, 3805−3806.
(5) Ma, Q.; Wooley, K. L. *J. Polym. Sci., Part A*: *Polym. Chem.* **2000**, *38*, 4805−4820.
(6) Becker, M. L.; Remsen, E. E.; Wooley. K. L. *J. Polym. Sci., Part A*: *Polym. Chem.* **2001**, *39*, 4152−4166.
(7) Ma, Q.; Remsen, E. E.; Kowalewski, T.; Wooley, K. L. *J. Am. Chem. Soc.* **2001**, *123*, 4627−4628.
(8) Sanji, T.; Nakatsuka, Y.; Kitayama, F.; Sakurai, H. *Chem. Commun.* **1999**, 2201−2202.
(9) Sanji, T.; Nakatsuka, Y.; Ohnishi, S.; Sakurai, H. *Macromolecules* **2000**, *33*, 8524−8526.
(10) Underhill, R. S.; Liu, G. *Chem. Mater.* **2000**, *12*, 2082−2091.
(11) Fujii, S.; Cai, Y.; Weaver, J. V. M.; Armes, S. P. *J. Am. Chem. Soc.* **2005**, *127*, 7304−7305.
(12) Butuen, V.; Wang, X.-S.; de Paz Banez, M. V.; Robinson, K. L.; Billingham, N. C.; Armes, S. P. *Macromolecules* **2000**, *33*, 1−3.
(13) Liu, S.; Armes, S. P. *J. Am. Chem. Soc.* **2001**, *123*, 9910−9911.
(14) Thurmond, K. B.; Kowalewski, T.; Wooley, K. L. *J. Am. Chem. Soc.* **1996**, *118*, 7239−7240.
(15) Huang, H.; Kowalewski, T.; Remsen, E. E.; Gertzmann, R.; Wooley, K. L. *J. Am. Chem. Soc.* **1997**, *119*, 11653−11659.
(16) Zhang, Q.; Remsen, E. E.; Wooley, K. L. *J. Am. Chem. Soc.* **2000**, *122*, 3642−3651.
(17) Butuen, V.; Billingham, N. C.; Armes, S. P. *J. Am. Chem. Soc.* **1998**, *120*, 12135−12136.
(18) Butuen, V.; Lowe, A. B.; Billingham, N. C.; Armes, S. P. *J. Am. Chem. Soc.* **1999**, *121*, 4288−4289.
(19) Pilon, L. N.; Armes, S. P.; Findlay, P.; Rannard, S. P. *Langmuir* **2005**, *21*, 3808−3813.
(20) Liu, S.; Weaver, J. V. M.; Save, M.; Armes, S. P. *Langmuir* **2002**, *18*, 8350−8357.
(21) Stewart, S.; Liu, G. *J. Chem. Mater.* **1999**, *11*, 1048−1054.
(22) Li, Y.; Lokitz, B. S.; McCormick, C. L. *Macromolecules* **2006**, *39*, 81−89.
(23) Li, Y.; Lokitz, B. S.; Armes, S. P.; McCormick, C. L. *Macromolecules* **2006**, *39*, 2726−2728.
(24) Weaver, J. V. M.; Tang, Y. Q.; Liu, S.; Iddon, P. D.; Grigg, R.; Armes, S. P.; Billingham, N. C.; Hunter, R.; Rannard, S. P. *Angew. Chem., Int. Ed.* **2004**, *43*, 1389−1392.
(25) Sanada, F.; Endo, T. *Macromol. Chem. Phys.* **1999**, *200*, 2651−2661.
(26) Sanada, F.; Abe, T.; Endo, T. *J. Polym. Sci., Part A*: *Polym. Chem.* **1997,** *35*, 2619−2629.
(27) Mori, H.; Sutoh, K.; Endo, T. *Macromolecules* **2005**, *38*, 9055−9065.
(28) Matyjaszweski, K., Ed. *Controlled/Living Radical Polymerization;* American Chemical Society: Washington, DC, 2003.
(29) Hawker, C. J.; Bosman, A. W.; Harth, E. *Chem. Rev.* **2001**, *101*, 3661−3688.
(30) Matyjaszewski, K.; Xia, J. *Chem. Rev.* **2001**, *101*, 2921−2990.
(31) Moad, G.; Rizzardo, E.; Thang, S. H. *Aust. J. Chem.* **2005**, *58*, 379−410.
(32) Chiefari, J.; Chong, Y. K.; Ercole, F.; Krstina, J.; Jeffery, J.; Le, T. P. T.; Mayadunne, R. T. A.; Meijs, G. F.; Moad, C. L.; Moad, G.; Rizzardo, E.; Thang, S. H. *Macromolecules* **1998**, *31*, 5559−5562.
(33) Perrier, S.; Takolpuckdee, P. *J. Polym. Sci., Part A: Polym. Chem.* **2005,** *43*, 5347−5393.
(34) McCormick, C. L.; Lowe, A. B. *Acc. Chem. Res.* **2004**, *37*, 312−325.
(35) Sumerlin, B. S.; Donovan, M. S.; Mitsukami, Y.; Lowe, A. B.; McCormick, C. L. *Macromolecules* **2001**, *34*, 6561−6564.
(36) Sumerlin, B. S.; Lowe, A. B.; Thomas, D. B.; McCormick, C. L. *Macromolecules* **2003**, *36*, 5982−5987.
(37) Vasilieva, Y. A.; Thomas, D. B.; Scales, C. W.; McCormick, C. L. *Macromolecules* **2004**, *37*, 2728−2737.
(38) Donovan, M. S.; Lowe, A. B.; Sanford, T. A.; McCormick, C. L. *J. Polym. Sci., Part A*: *Polym. Chem.* **2003**, *41*, 1262−1281.

(39) Donovan, M. S.; Sumerlin, B. S.; Lowe, A. B.; McCormick, C. L. *Macromolecules* **2002**, *35*, 8663−8666.
(40) Donovan, M. S.; Sanford, T. A.; Lowe, A. B.; Sumerlin, B. S.; Mitsukami, Y.; McCormick, C. L. *Macromolecules* **2002**, *35*, 4570−4572.
(41) Thomas, D. B.; Sumerlin, B. S.; Lowe, A. B.; McCormick, C. L. *Macromolecules* **2003**, *36*, 1436−1439.
(42) Convertine, A. J.; Ayres, N.; Scales, C. W.; Lowe, A. B.; McCormick, C. L. *Biomacromolecules* **2004**, *5*, 1177−1180.
(43) Mitsukami, Y.; Donovan, M. S.; Lowe, A. B.; McCormick, C. L. *Macromolecules* **2001**, *34*, 2248−2256.
(44) Convertine, A. J.; Lokitz, B. S.; Vasileva, Y.; Myrick, L. J.; Scales, C. W.; Lowe, A. B.; McCormick, C. L. *Macromolecules* **2006**, *5*, 1724−1730.
(45) Thomas, T. B.; Convertine, A. J.; Myrick, L. J.; Scales, C. W.; Smith, A. E.; Lowe, A. B.; Vasiliva, Y. A.; Ayres, N.; McCormick, C. L. *Macromolecules* **2004**, *37*, 8941−8950.
(46) Camail, M.; Margaillan, A.; Maesano, J. C.; Thuret, S.; Vernet, J. L. *Polymer* **1998**, *39*, 3187−3192.
(47) Heskins, M.; Guillet, J. E. *J. Macromol. Sci., Chem.* **1968**, *A2*, 1441−1455.
(48) Cho, E. C.; Lee, J.; Cho, K. *Macromolecules* **2003**, *36*, 9929−9934.
(49) Yusa, S.; Shimada, Y.; Mitsukami, Y.; Yamamoto, T.; Morishima, Y. *Macromolecules* **2004**, *37*, 7507−7513.
(50) Liu, B.; Perrier, S. *J. Polym. Sci., Part A: Polym. Chem.* **2005**, *43*, 3643−3654.
(51) Xia, Y.; Yin, X.; Burke, N. A. D.; Stover, H. D. H. *Macromolecules* **2005**, *38*, 5937−5943.
(52) Greenwood, R. *Adv. Colloid Interface Sci.* **2003**, *106*, 55−81.
(53) Sumerlin, B. S.; Lowe, A. B.; Thomas, D. B.; Convertine, A. J.; Donovan, M. S.; McCormick, C. L. *J. Polym. Sci., Part A: Polym. Chem.* **2004**, *42*, 1724−1734.

MA061672Y